Options for Monitoring Land Subsidence Data in Victoria County, Texas

Prepared for:

Victoria County Groundwater Conservation District

Prepared by:

INTERA Incorporated
9600 Great Hills Trail
Suite 300W
Austin, TX 78759
512.425.2000

June 2019

This page intentionally left blank.

Options for Monitoring Land Subsidence Data for Victoria County, Texas

Prepared By

Steve C. Young, Ph.D., P.G., P.E.

This page intentionally left blank.

TABLE OF CONTENTS

LIST OF FIGURES

LIST OF TABLES

Acronyms and Abbreviations

ASR	aquifer storage and recovery
BCGCD	Brazoria County Groundwater Conservation District
CORS	Continuously Operating Reference Station
DEM	Digital Elevation Model
FAA	Federal Aviation Administration
FBSD	Fort Bend Subsidence District
GCD	groundwater conservation district
GMA	groundwater management area
GNSS	global navigation staellite system
GPS	global positioning system
HGSD	Harris-Galveston Subsidence District
IMU	Inertial measurement unit
INsar	Interferometric Synthetic Aperture Radar
LiDAR	Light Detection and Ranging
LSGCD	Lone Star Groundwater Conservation District
m	meters
NAVD88	North American Vertical Datum
NGS	National Geodetic Survey
NOAA	National Oceanic and Atmospheric Administration
PAM	Port-A-Measure
PID	Permanent IDentifier
SAR	synthetic aperture radar
TCEQ	Texas Commission on Environmental Quality
TIN	Triangulated Irregular Network
TXDOT	Texas Department of Transportation
USGS	United States Geological Survey
VCGCD	Victoria County Groundwater Conservation District

1.0 INTRODUCTION

This report describes techniques for measuring land subsidence that have been used in the Houston area in Texas and the central basin in California. The report expands on information regarding historical estimates of land subsidence in seven groundwater conservation districts in Groundwater Management Area (GMA) 15 documented in Young, 2016. The objectives of the report are to:

- Describe the techniques to measure land subsidence;
- Compare the benefits and costs associated with the different measurement techniques;
- Evaluate options for application by VCGCD; and
- Develop costs for a plan to measure land subsidence in Victoria County

The report is organized into five sections. Section 1 introduces the study and lists the study's objectives. Section 2 reviews the mechanisms that cause land subsidence. Section 3 describes techniques that have been used to measure land subsidence. Section 4 provides a monitoring approach design for consideration by VCGCD. Section 5 provides references cited in this report.

2.0 INTRODUCTION TO LAND SUBSIDENCE

This section provides a general introduction to the mechanisms that cause land subsidence and summarizes the extent of land subsidence in the Harris-Galveston area.

2.1 Introduction to Land Subsidence

Among the first studies to recognize that land subsidence could be caused by depressurization of aquifers by pumping were Meinzer and Hard (1925). Meinzer and Hard (1925) recognized that a confined aquifer (the Dakota Sandstone) was compressed when the hydraulic head was decreased. They reported that the overburden pressure from all deposits above the confined Dakota Aquifer was supported partly by the fluid pressure within the Dakota and partly by the sandstone itself (grain-to-grain load).

Meinzer formulated his land subsidence theory in 1928 in a classic paper (Meinzer, 1928), which discusses the compressibility and elasticity of aquifers. He cited evidence for compressibility and elasticity derived from laboratory tests and from field evidence for confined aquifers and for large artesian basins, notably the Dakota artesian basin. He concluded:

> "...aquifers are apparently all more or less compressible and elastic though they differ widely in the degree and relative importance of these properties. In general the properties of compressibility and elasticity are of the most consequence in aquifers that have low permeability, slow recharge, and high head. In many aquifers these properties are evidently important in supplying water not only by permanent reduction of storage but also by temporary reduction that is replenished when the wells are shut down or during the season of minimum use."

An important consideration regarding how depressurization will affect the compressibility of the aquifer is the distribution of clays and sands within the aquifer. Clays are orders of magnitude more susceptible to compression than sands (Freeze and Cherry, 1979; Domenico and Schwartz, 1990). In fact, the difference between clays and sands is so large that the compressibility of the sands is sometimes ignored in the calculation of land subsidence.

The large difference in compressibility between sands and clays occurs because sands and clays have dissimilar shaped grains and dissimilar grain-to-grain geometry. Whereas sand grains are round-like structures, clay grains are flat-like structures. The difference in shape between sands and clays affects how they consolidate in response to increased effective stress. **Figure 2-1** is a schematic showing how sand grains mechanically compress differently than clay grains. Mechanical compression occurs as a result of slippage and rotation that change the position and orientation of individual grains and does not involve the actual compression of the individual grains. Because of the plate-like shape, clay grains can pack closer together than sand grains. After compaction, the porosity in sands typically ranges between 0.25 and 0.4, whereas the porosity of clays typically ranges between 0.05 and 0.1 (Revil and others, 2002). At the time of their deposition, clays typically have higher porosities than sands. Therefore, the potential reduction in porosity caused by compressibility from the time of deposition to consolidation is significantly greater for clays than for sands. This is because of the compressibility of clay versus sand.

2.2 Land Subsidence in United States and the Houston Area

Subsidence is a global problem and, in the United States, more than 17,000 square miles in 45 states, an area roughly the size of New Hampshire and Vermont combined, have been directly affected by subsidence (Galloway and others, 1999) The principal causes are aquifer-system compaction, drainage of organic soils, underground mining, hydrocompaction, natural compaction, sinkholes, and thawing permafrost (National Research Council, 1991). The compaction of unconsolidated aquifer systems that can accompany excessive ground-water pumping is by far the single largest cause of subsidence. The overdraft of such aquifer systems has resulted in permanent subsidence and related ground failures. In aquifer systems that include semi-consolidated silt and clay layers (aquitards) of sufficient aggregate thickness, long-term ground-water-level declines can result in a vast one-time release of "water of compaction" from compacting clays and resulting land subsidence.

One of the aquifers most susceptible to land subsidence in Texas is the Texas Gulf Coast Aquifer (Furnans and others, 2018). The vulnerability of the Gulf Coast Aquifer is attributed to historically and anticipated high groundwater pumping and the relatively young Miocene deposits that comprise the Chicot and Evangeline Aquifers. These deposits are unconsolidated, under consolidated, and contain appreciable clays. Land subsidence in the Houston, Texas area has been occurring for almost a century. Since the mid-1950s, the USGS and cooperating agencies have placed an emphasis on collecting and analyzing groundwater-elevation data in the Harris-Galveston Region because of concerns about land subsidence. A historical review of these activities is discussed by Gabrysch (1982), Gabrysch and Coplin (1990), and Gabrysch and Neighbors (2000, 2005). Accumulated subsidence of over 3 meters (m) during the past century has been observed in a large area of southeast Harris County, including Houston downtown, the cities of Pasadena, Baytown, Texas City, and Galveston (Kasmarek and others, 2009).

Figure 2-2 shows a map of land subsidence estimated to have occurred from 1906 to 2000 in the Houston Area. Most of the subsidence in the Houston area has occurred as a direct result of groundwater withdrawal from the Chicot and Evangeline aquifers (Coplin and Galloway, 1999; Kasmarek and others, 2014; Kearns and others, 2015). **Figure 2-3** illustrates pumping from 1890 to 2004 that has occurred in the Harris-Galveston area. To prevent land subsidence, the Texas Legislature created the Harris-Galveston Subsidence District (HGSD) in 1975, the Fort Bend Subsidence District (FBSD) in 1989, the Lone Star Groundwater Conservation District (LSGCD) in 2001, and the Brazoria County Groundwater Conservation District (BCGCD) in 2003. One of the primary obligations of these districts is to regulate and reduce groundwater withdrawal for the purpose of minimizing land subsidence, which contributes to infrastructure damage and flooding.

2.3 Land Subsidence in Victoria County

Ratzlaff (1982) evaluated land subsidence in the Texas coastal region by comparing adjusted elevations of benchmarks for various periods of releveling and by comparing topographic maps of the same area for different years. His primary set of benchmark elevations was published by the National Geodectic Survey (NGS), with additional elevations obtained from the Texas Department of Highways and Public Transportation and the Texas Department of Water Resources. Ratzlaff (1982) discusses land subsidence in Victoria County only in the southeast area near the boundary of Jackson County. In southeast Victoria County, Ratzlaff (1982) reports land subsidence is 0.5 ft or less. According to Ratzlafff (1982):

> "The large area of subsidence in the eastern one-half of Jackson County and the northwestern part of Matagorda County, most of which occurred between 1950 and 1973, is the result of declines in water levels resulting from an increase in ground-water withdrawals for irrigation in the early 1950's (Loskot and others, 1982). The area of subsidence extending westward from Jackson County into Victoria County is also the result of an increase in ground-water withdrawals for irrigation.
>
> Land-surface subsidence in southeastern Victoria County is probably related to oil and gas production. There are very few water wells and only a small amount of ground-water withdrawals in the subsided area. Water levels in observation wells within the subsided area declined more than 1 foot (0.3 m) from 1958 to 1973 (Texas Department of Water Resources, unpublished data); but these declines were not sufficient to cause the subsidence shown for the area."

In 2016, several GCDs in GMA 15 funded a study by INTERA Inc. (Young, 2016) to use publicly available data to estimate historical land subsidence. Young (2016) estimated historical land subsidence from several available data sets. The most reliable estimates of land subsidence were calculated using the (NGS) network of Permanent Identifiers (PIDS) and LIght and raDAR (LIDAR) that was obtained from the Texas Natural Resources Information System (TNRIS). For the comparison, Young (2016) used measured elevation associated with the PIDs before 1950 and LIDAR measurements after 2006.

Because of a concern regarding unrepresentative land subsidence values calculated at some PID locations, Young (2016) divided the PIDs locations into groups so that statistical analysis could be performed to help eliminate the influence of improper or unrepresentative estimates of land subsidence. With considerations for similar values and for county borders, the PID locations were grouped into 54 polygons. Except for on polygon, all of the polygons except have an area greater than 40 square miles. **Figure 2-4** shows the median and average values of land subsidence for each polygon. Because of the occurrence of outliers in most of the polygons, the averages were calculated using only values falling above the 25th percentile and below the 75th percentile.

For Victoria County, Figure 2-4 indicates that no historical land subsidence has occurred in the northern west of the City of Victoria. For most of the county southeast of the City of Victoria, Figure 2-4 indicates that land subsidence between 0.2 and 0.8 ft has occurred.

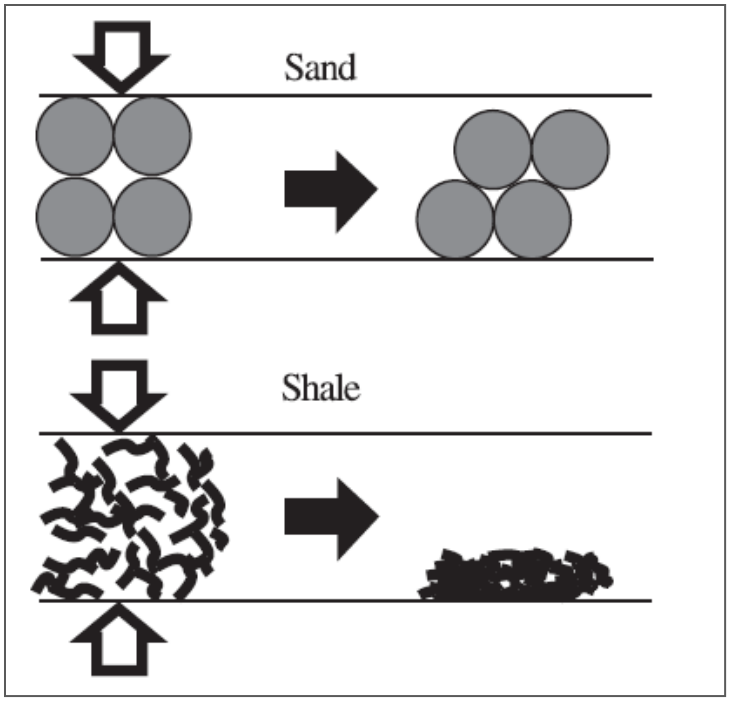

Figure 2-1 Schematic showing the reorientation and shifting of sand grains and shale comprised of clay particles associated with compaction caused by increased effective stress on the grain-grain contact

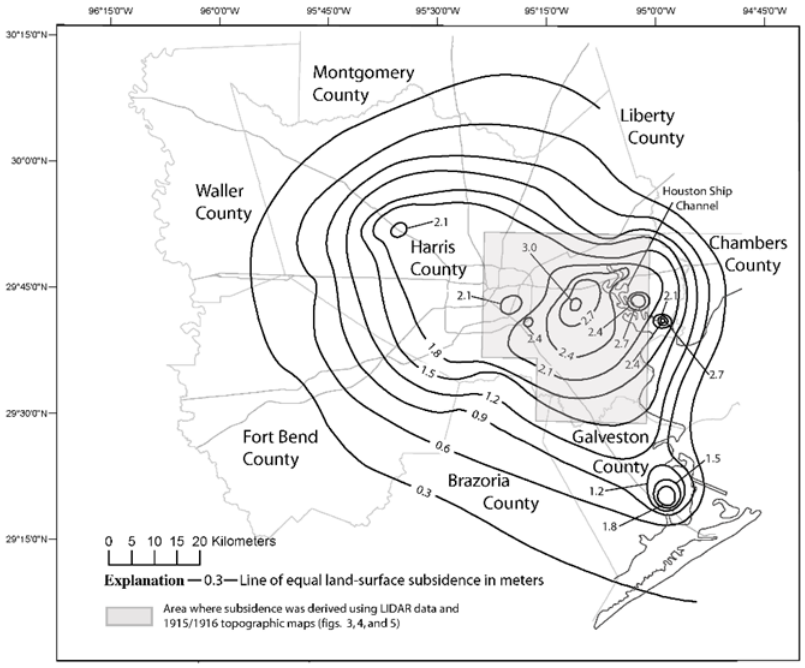

Figure 2-2 Approximate land-surface subsidence, 1906-2000 as reported by Gabrysch and Neighbors (2005)

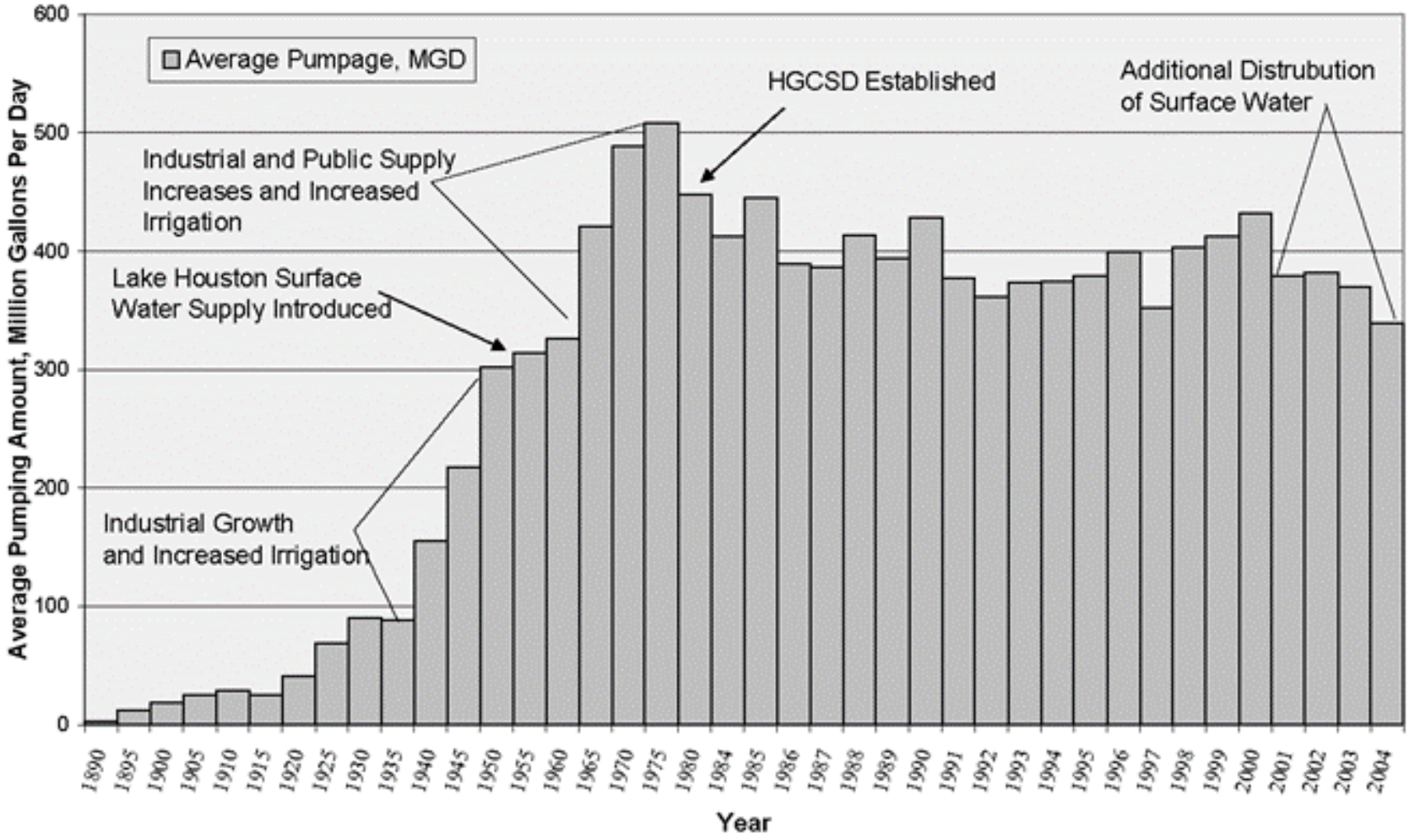

Figure 2-3 Historical pumping of groundwater in the Harris-Galveston Area (from Seifert and Drabek [2006])

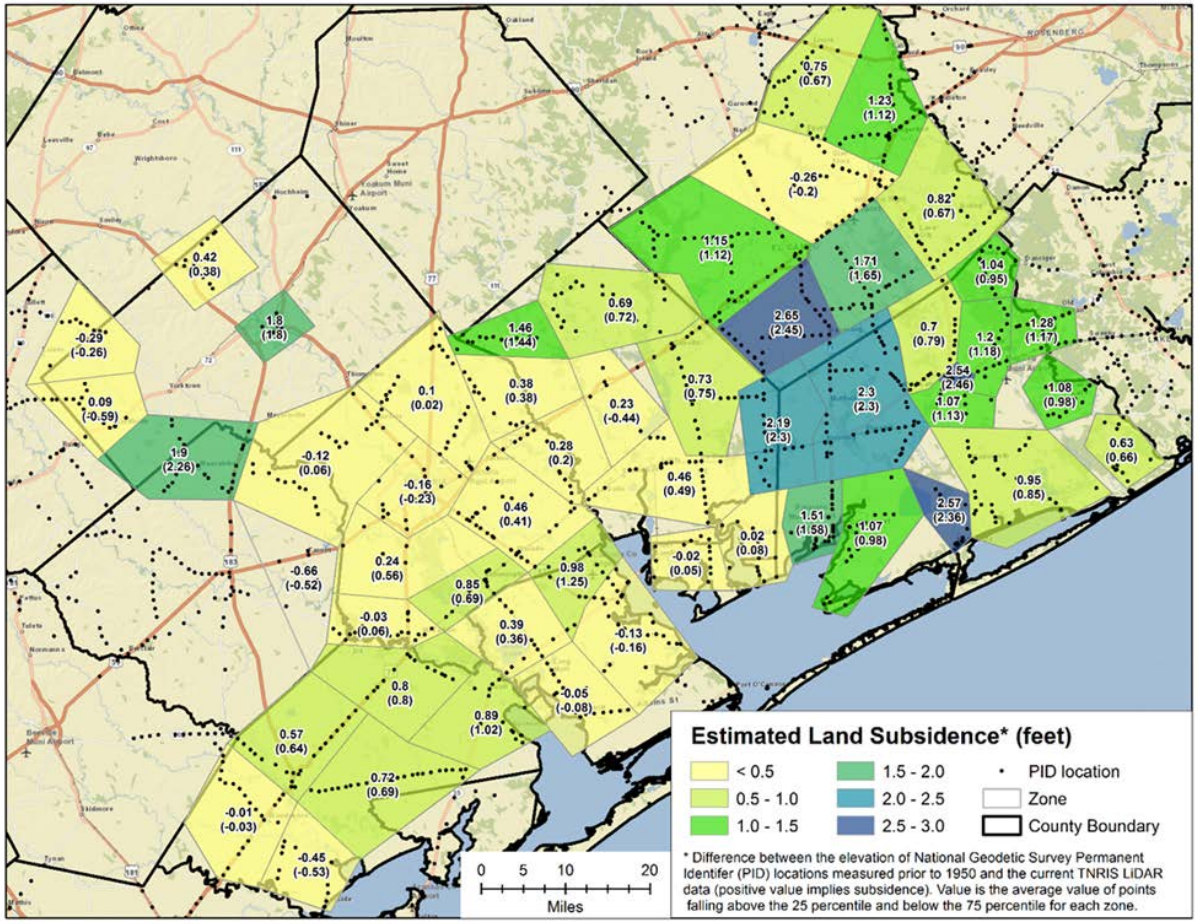

Figure 2-4 Estimated average land subsidence from before 1950 to after 2003 for specific polygons as determined by the difference between ground surface elevation from PIDs surveyed prior to 1950 and from LIDAR surveys after 2006 at the locations of the PIDs. Land Subsidence values are expressed as averages and medians (in parenthesis) of the differences calculated at PIDS located inside the polygons. Positive values indicate lower ground surface elevation at later time. Negative values indicate higher ground surface elevation at later time(from Young (2016)

3.0 TECHNIQUES FOR MONITORING LAND SUBSIDENCE

The monitoring of land subsidence in the Harris-Galveston area has been ongoing for almost a century, beginning with Pratt and Johnson (1926) documenting subsidence in the vicinity of the Goose Creek oil fields. Listed below is a summary of monitoring methods and their evolution through time.

3.1 Releveling Surveys

Prior to the advent of GPS technology, the standard practice for measuring land surface subsidence was to perform periodic releveling of surveyed benchmarks. The primary agency responsible for performing the releveling historically has been the United States Coast and Geodetic Survey (USC&GS) and its successor agency, the National Geodetic Survey (NGS). NGS releveling consists of conventional differential leveling at the highest accuracy level rating. Simple algebraic subtraction along level lines yields the land subsidence that occurred between any two releveling events. The subsiding benchmarks from surveys taken at different times (level line or spirit leveling) must be referenced to a common, highly stable benchmark in a non-subsiding area (American Geophysical Union, 1984). Survey benchmark re-leveling typically has a vertical resolution of less than 0.04 inches (Bawden and others, 2003). In areas where re-leveling survey benchmark data indicate subsidence, empirical relationships can be established between ground surface elevation changes and contributing factors (water level declines, clay thickness/depth, etc.).

The NGS provides historic records of these survey marks (including common highly stable benchmarks). These survey marks can be queried and downloaded from the NGS web page (https://www.ngs.noaa.gov/), where the data can be retrieved as either data sheets (text files with 80 columns of rigorously formatted metadata) or ArcGIS shapefiles. The website provides detailed instructions for retrieval including an interactive map of the most recent survey marks.

All NGS benchmark control points have Permanent IDentifier (PID) associated with them. A PID for a control point does not change and consists of six alphanumeric characters, with any alpha characters being upper case, such as TX1098. Often, benchmark control points are represented in the field by a metal disk permanently affixed to a solid and stable surface, or less frequently by an existing structure such as a church spire or communication tower. For the evaluation of historical land subsidence in GMA 15, Young (2016) downloaded ground elevation data from approximately 2,200 PID locations. These included a total of 259 PIDs for Victoria County. Out of these 259, only three of the PIDs have information after 1980.

A releveling event performed by the HGSD before the late 1980s involved about 2,500 locations and cost about $1,170,000 (2001 dollars) (Zilkoski and others, 2003). The high cost of a releveling events partly accounts for the lack of releveling epochs across much of the Gulf Coast since the 1950s.

3.2 Extensometers

One of the first techniques employed in the region, and possibly the most accurate when calculating compaction (Zilkoski and others, 2001), was the implementation of deep borehole extensometers. An extensometer consists of a borehole that contains a standpipe that can move vertically within a slip-

jointed casing (Gabrysch, 1984). Extensometers can be considered as deeply anchored benchmarks. **Figure 3-1** shows a schematic of a borehole extensometer. Borehole extensometers provide a continuous, 0.01-inch accuracy, measurement of vertical subsidence (American Geophysical Union, 1984).

The construction of an extensometer begins with drilling a borehole to a depth at which the strata are considered stable. In the Harris-Galveston area, the base of the Evangeline Aquifer has traditionally been assumed to be stable. The borehole is then lined with a steel casing with slip-joints to prevent it from crumpling as subsidence occurs. An inner pipe rests on a concrete plug at the bottom of the borehole and extends to the top. This inner pipe then transfers the stable elevation below to the surface. A measurement of the distance from the inner pipe to the surrounding land surface provides the amount of compaction that has occurred. A chart recorder provides a continuous record of subsidence over time.

The USGS began installing extensometers in the Harris-Galveston region in the early 1960s. Borehole extensometers provide excellent subsidence data, but their high cost prohibits their use in sufficient numbers to provide adequate information for an entire study area. Zilkoski and others (2003) estimate the average cost of an extensometer at approximately $800,000 in 2001 dollars.

3.3 GPS–based Methods

Global Positioning System (GPS) is defined as a navigational system using satellite signals to fix the location of a radio receiver on or above the ground surface. In 1993, the HGSD and the NGS signed a cooperative agreement to jointly pursue an experimental study using a GPS to measure subsidence. The rationale for the GPS system was to both improve the quality and reduce the price associated with using re-leveling surveys to monitor land subsidence in the Houston area. The HGSD started utilizing GPS in its study of regional subsidence in 1994. (Neighbors and Mitchell, 2010).

The HGSD employs both fixed and mobile GPS stations The fixed location setups are called Continuously Operating Reference Stations (CORS). The mobile GPS setups are called Port-A-Measure (PAM) stations. The first three GPS stations were CORS that were installed on the extensometers. In 2014, there were approximately 40 CORS (Wang and others, 2015) and approximately 80 PAMS (Wang and others, 2015) in the Houston Area. As of 2017, Kearns and others, (2018) reports that there are approximately 200 permanent GPS stations within the greater Houston area

3.3.1 Continuous Operating Reference Stations

In the Houston area, the CORS are operated by a joint effort of the NGS at the National Oceanic and Atmospheric Administration (NOAA), the Texas Department of Transportation (TXDOT), the City of Houston, and other local agencies. CORS provide the Global Navigation Satellite System (GNSS) data consisting of carrier phase and code range measurements in support of three dimensional positioning, meteorology, space weather, and geophysical applications throughout the United States. The CORS network is a multi-purpose cooperative endeavor involving government, academic, and private organizations. The sites are independently owned and operated. Each agency shares their data with NGS, and NGS in turn analyzes and distributes the data free of charge.

Surveyors, GIS users, engineers, scientists, and the public at large that collect GPS data can use CORS data to improve the precision of their positions. CORS enhanced post-processed coordinates approach a few centimeters relative to the National Spatial Reference System, both horizontally and vertically. The GNSS data collected at these stations are made available to the public by NGS. The data include observation, meteorological, navigation/ephemeris, station logs and NGS coordinate files for the stations. Most data are available within one hour from when they were recorded at the remote site, and a few sites have a delay of 24 hours. **Figure 3-2** shows the location of CORS sites near the City of Victoria.

The CORS in Victoria County is located at latitude 28.83493° N and longitude is 96.9096°W and is maintained by TXDOT. Information regarding the location and measurements of land surface change over time is available at https://geodesy.noaa.gov/CORS/. The available information includes movement in the east, north, and vertical direction **Figure 3-3** shows the changes in the elevation of the station. The cyclic pattern in the elevation change is seasonal and ranges approximate ± 20 mm.

3.3.2 Port-A-Measure Stations

A PAM station was designed for a campaign-style long-term monitoring solution. A PAM Station originally included a trailer, its own power supply, a cellular phone, and a permanently install 2.5-m (8-foot) antenna pole (**Figure 3-4**). To avoid the impact of surface ground deformation associated with the shrink-swell behavior of clay-rich soils in the Houston area, the antenna poles were anchored 6 m below the ground surface. **Figure 3-5** shows a design for a typical PAM stations that is s composed of three parts, of which two parts are placed into a 6-meter deep drilled hole The lower part, made of sakrete-mix of concrete, provides the stability of the monument. Above the sakrete concrete part, the 2-1/2 inch PVC (polyvinyl chloride) sleeve is set. This PVC part is stabilized using one bag of sakrete around the sleeve. The third part of the monument, on the land surface, is cemented on the PVC sleeve. This part is a heavy wall galvanized pipe 2.5 meter (8 feet) high.

The PAM units use dual-frequency, full-wavelength GPS instruments (with geodetic antennas) to collect data that provide daily land subsidence measurements with a vertical accuracy of “plus or minus” one centimeter. HGSD and FBSD personnel routinely mount GPS antennas on permanent antenna poles to monitor land subsidence. On average, GPS data were collected continuously for one week every month prior to 2005 and one week per two months after 2005.The PAM network has been continuously expanded and the number of total stations has reached over 90 in the Houston metropolitan area as of 2017 (Kearns and others, 2018).

With assistance from the HGSD, BCGCD has installed seven PAM stations in theirdistrict in 2016. **Figure 3-6** shows one of the PAMs installed by BCGCD. As a result of current improvement in GPS equipment, the trailer is no longer an essential PAM component. In addition, the PAM stations are permanent fixtures. The mobile component of the PAM stations is the GPS equipment.

Costs associated with installation PAM stations can be estimated based on BCGCD installation of seven PAM stations in 2016 to 2017. The cost of installation of the seven stations was approximately $42,000. The costs for installation another seven PAM stations is 2019 is still approximately $42,000. The company used to install the station is Davison Water Well Service , who are headquartered in Brazoria County. We anticipate that installations of PAM installation in Victoria County could be notably greater that those for BCGCD because of additional mobilization costs for Davison Water Well Service if they

were used or because of the learning curve another drilling firm located closer to Victoria County would have. BCGCD is currently collect data from their seven PAM stations by rotating a single GPS unit, which costs approximately $5,000. The GPS unit remains at a station for approximately a week before the data is downloaded and the GPS unit is moved to another PAM station. The data processing and web hosting of the change in ground location and elevation is performed by HGSD. The estimated costs for the data management services is approximately $7,500 per year.

3.4 Remote-Sensing Methods

Remote sensing is the process of detecting and monitoring the physical characteristics of an area by measuring its reflected and emitted radiation at a distance from the targeted area. Remote sensing technologies typically gather information about the surface of the earth from a distant platform, usually a satellite or airborne sensor about the Earth. Two remote sensing methods used to map the differences in the elevation of the ground surface over time is LiDAR and INSAR.

3.4.1 LIDAR

Airborne laser scanning, also commonly known by the acronym LiDAR (Light Detection And Ranging) is an active remote sensing technique that measures distance by illuminating a target with a laser and analyzing the reflected light. The laser emits tens of thousands of pulses per second. To obtain measurements for the horizontal coordinates (x, y) and elevation (z) of the objects scanned, the position of the aircraft is determined using accurate GPS measurements. LiDAR has been used extensively both in tripod-mounted ground scanning and in airborne mapping surveys. LiDAR collects measurements independent of weather conditions or time of day, but it is limited to line-of-sight measurements unless a target is scanned from different vantage points. The LiDAR data are result of: (i) the time difference between the emitted and returned laser pulses, (ii) the angle of the source, and (iii) the location of the sensor (NOAA, 2008).

Figure 3-8 shows a schematic of the components associated with an airborne LiDAR system. The four primary components of any LiDAR system are:

- **LiDAR sensors** scan the ground from side to side as the plane flies. The sensor is commonly in green or near-infrared bands;
- **GPS receivers** track the altitude and location of the airplane. These variables are important in attaining accurate terrain elevation values;
- **Inertial measurement units (IMU)** tracks the tilt of the airplane as it flies. Elevation calculations use tilt to accurately measure incident angle of the pulse;
- **Computers (Data Recorders)** record all of the height information as the LiDAR scans the surface.

There are many potential sources of error in elevations acquired by LiDAR measurements: LiDAR equipment, interpolation, horizontal displacement, flight height, terrain slope, and ground cover all influence LiDAR-determined elevations (Hodgson and Bresnahan, 2004). Airborne LiDAR measurements have a lower vertical resolution compared to other methods of measuring the elevation of the land surface. Tripod mounted LiDAR provides distance from the instrument to the land surface with a resolution of at least 0.39 inch (Borchers and Carpenter, 2014) based on travel time (Fowler, 2001).

In addition to providing dense data across large areas of open terrain, LiDAR is distinguished from other remote sensing technologies by its ability to provide data from terrain and objects under forest canopy. As a lidar sensor is flown over a forested, woodland or scrub landscape area, some returns will penetrate the vegetation canopy, reach the ground, and return to be recorded by the sensor- effectively allowing the creation of terrain models as seen through vegetation (NOAA, 2008). This property of LiDAR is both an advantage and a disadvantage for creating a bare-earth surface with respect to the vegetation density. The bare-earth surface is a model that is created by the returns reflected from the ground directly. To differentiate this return from others reflected from buildings or vegetation, some filtering methods are applied (Sithole & Vosselman, 2004). The way of classifying returns is to use the GIS location of the buildings and aerial photos (Engelkemeir & Khan, 2008). Digital Elevation Models (DEMs) are generated from the bare-earth data of LiDAR. The DEM is created by using Triangulated Irregular Network (TIN) which has neither overlaps nor space while generating the grids of DEM (Engelkemeir, 2010).

Karacay (2013) and Khan and others (2014) report on the same application of using LiDAR data to determine land subsidence in northwest Harris County. The application involves using LiDAR datasets from 2001 and 2008. The report accuracy of the LiDAR datasets were with horizontal accuracy ±75 cm for 2001 data and ±70 cm for 2008 data. The vertical datum is North American Vertical Datum 1988 (NAVD88) with the accuracy ±15 cm and ±9.25cm for 2001 and 2008 data, respectively. The analysis of the LiDAR data showed land subsidence from 0.3 to 4.5 cm/yr. These results were consistent with land subsidence produced by the analysis of GPS data and InSAR data.

In order to develop a cost estimate for obtaining LIDAR data in Victoria County, we contacted two commercial firms – one near the City of Bryan and the other near San Antonio for pricing information. The cost estimate to survey a 400 acre parcel and a 200 acre parcel was approximately $16,000, which is about $27/acre. The LiDAR data will have an accuracy of 2 cm and 5 cm in the horizontal and vertical, directions. The LIDAR data will be configured into a Digital Elevation Model (DEM) of topography delivered on a 1 ft by 1 ft grid. The DEM will have vertical resolution of 3-inches.

3.4.2 SAR and InSAR

A promising remote sensing technique other than GPS for measuring land subsidence is called Satellite Aperture Radar (SAR). Among the attractive characteristics of SAR is its ability to monitor larger areas than a specific point (Bawden and others, 2012). SAR can provide more detailed subsidence mapping over larger areas than can be measured by any other remote sensing techniques or GPS techniques. Measurements can be done entirely retroactively, by acquiring historic (1992 to present) repeat SAR data sets for the area of interest, and then processing the SAR data using interferometric techniques to determine changes in elevation over large areas with a precision of a few millimeters.

Taking multiple SAR scans of a region and differencing (or interfering) them is known as Interferometric Satellite Aperture Radar (InSAR). InSAR is effective at quantifying all points in a region (i.e., the entire county and not a single point). Under ideal conditions, InSAR can detect surface deformation of less than half an inch over hundreds of square miles, at a horizontal spatial resolution of 295 feet or better (Sneed and others, 2013). Radar signals generated from a satellite are bounced off stable radar reflectors on the Earth's surface, such as roads, buildings, other engineered structures, mountains, and undisturbed ground and rocks. The travel time of the radar signal from the satellite to the ground and back to the

satellite is proportional to the distance between the satellite and the ground. Subtracting, or interfering, the data collected by a satellite passing over the Earth at different times provides the information needed to prepare interferograms and interpret subsidence magnitude.

The InSAR technique has been used extensively to study groundwater systems and land subsidence (Chen and others, 2017; Hoffmann and others, 2001; Miller & Shirzaei, 2019; Reeves and others, 2011; Smith and others, 2017; Smith and others, 2019). Results from example application of InSAR for estimating land subsidence is provided in Appendix A. Several studies have successfully used InSAR to map land subsidence in the Houston Area (Buckley and others, 2003; Casu and others, 2005; Bawden and others, 2012; Qu and others 2015; Miller and Shirzaei, 2019). Several of the studies discussed that one of environment conditions that can limit the and complicate the application of InSAR in the Houston-Galveston region was atmospheric moisture associated with clouds. In general, atmospheric moisture delays the radar signal as it travels from the satellite to the ground and back. This delay increases the radar signal travel time and the calculated range distance and can produce artifacts in the analysis. In order to mitigate the error associated with atmospheric moisture, advanced filtering routines are needed (European Space Agency, 2007).

In order to develop cost estimate for processing InSAR data from Victoria County, we contacted commercial firms and several research institutes including universities. The consulting firms that we contacted were highly specialized and were not interested in a speculative project that is likely less than $25,000. Two academics were interested in the possibility of performing the Phase 1 work. One of these academics is Dr. Zhong Lu. Dr. Lu is the Shuler-Foscue Endowed Chair Professor the Huffington Department of Earth Science, at Southern Methodist University in Dallas Texas. The other academic is Dr. Shuhab Khan. Dr. Khan operates the Geosceinces Remote Sensing (GeoRS) Facility at the University of Houston. Both Dr. Khan and Dr. Lu agreed to perform the analysis of InSAR data for Victoria County for about $15,000 . The InSAR data that is available for Victoria County includes the following periods mid-1990s to 2000; 2007-2011, and 2015-present.

3.4.3 Summary of Monitoring Approaches

The technologies available to monitored land subsidence has advanced significantly since releveling surveys were used extensively in the early 1970s in the Houston-Galveston. During the last forty years, the Houston-Galveston area has advanced into one of the areas in the world most intensively monitored for land subsidence. From a scientific perspective, the monitoring activities have been a well spring for testing and cross-validating different techniques and approaches for measuring land subsidence. In our opinion, all of the methods discussed above provide sufficient accuracy for the purpose of detecting whether or not notable land subsidence has or is occurring. The primary differentiator is costs, what is the highest level of accuracy that can be achieved with the measurement, and the spatial resolution, and the complexity associated with the data analyses. For the purpose of evaluating the different methods for application by VCGCD, **Table 3-1** has been created.

Table 3-1 Subsidence monitoring methods

Method	Deliverable/ (Comment)	Spatial Coverage	Temporal Coverage	Relative Cost
Borehole Extensometers	Accurate monitoring of vertical land surface elevation changes (capable of providing compaction data for different aquifers if multiple extensometers are	Point	Continuous future subsidence measurement	Very High
Survey Benchmark Re-leveling	Accurate measurement of vertical ground movement (susceptible to human errors with measuring and managing data)	Line	Specific Survey dates measurement	Medium to High
LiDAR	Highly detailed elevation model of ground surface (does not provide a direct method for monitoring horizontal movement)	Area	Specific Survey dates (no satellite data available)	Medium to High
High Accuracy GPS Network	Measurement of vertical and horizontal ground movement (relatively simple to collect and analyzed data)	Point	Continuous or repeat future land movement measurement	Low to high (dependent on accuracy, frequency, and number of locations)
InSAR Data Collection	Accurate measurement of vertical land movements (accuracy affected by high cloud cover and dense vegetation)	Area	Repeat future vertical land movement measurement	Low to medium (freely available data may require specialized data processing)

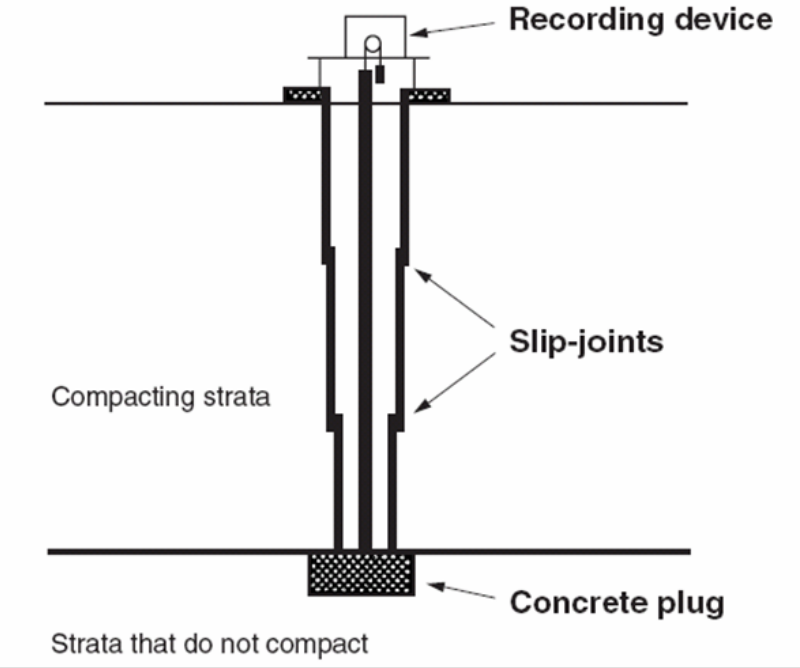

Figure 3-1 Schematic of a borehole extensometer used by the Harris-Galveston Coastal Subsidence District (modified from Zilkoski and others, 2003).

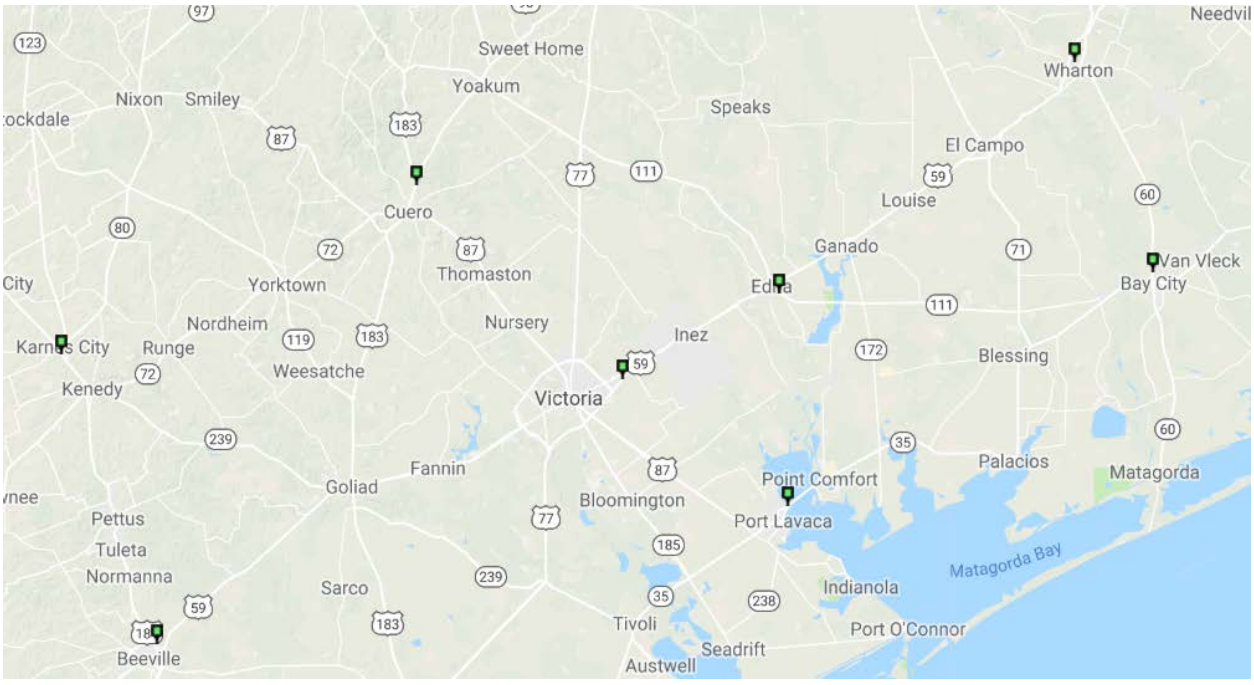

Figure 3-2 Location of continuous operating reference stations (CORS) in the vicinity of Victoria County (from https://www.ngs.noaa.gov/CORS/). Sites are shown a green boxes outlined in black.

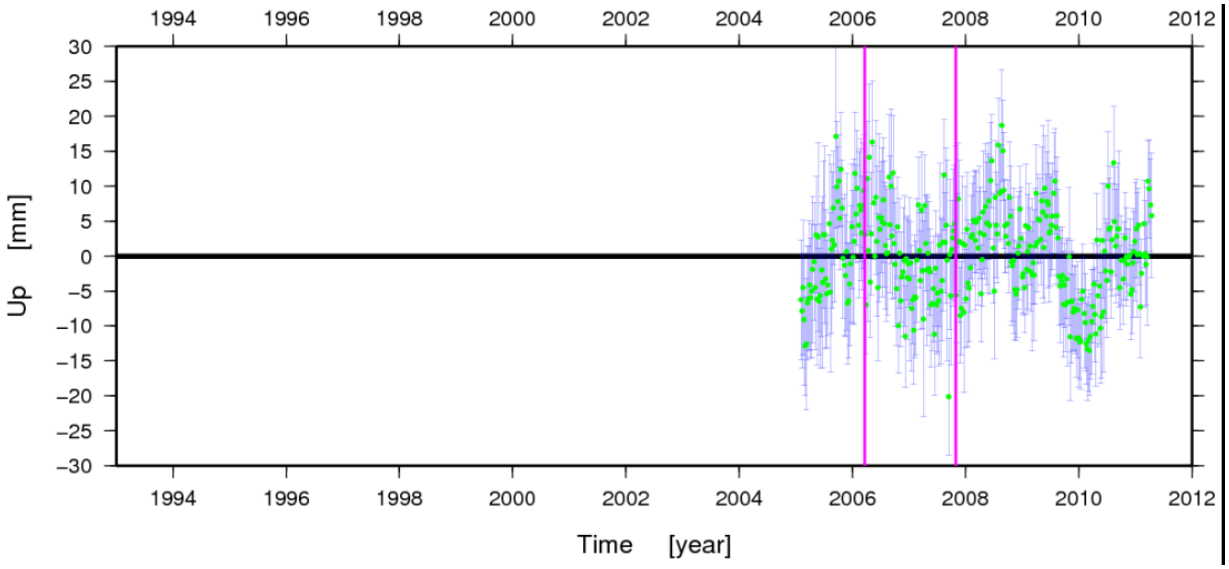

Figure 3-3 Change in elevation at land surface at COR station TXVA in Victoria County near City of Victoria (see Figure 3-3) , obtained from https://geodesy.noaa.gov/cgi-cors/corsage_2.prl?site=TXVA.

Figure 3-4 Picture of a Port-A-Measure (PAM) GPS antenna (modified from Zilkoski and others, 2003, obtained from https://hgsubsidence.org/frequently-asked-questions/measurement-FAQs)

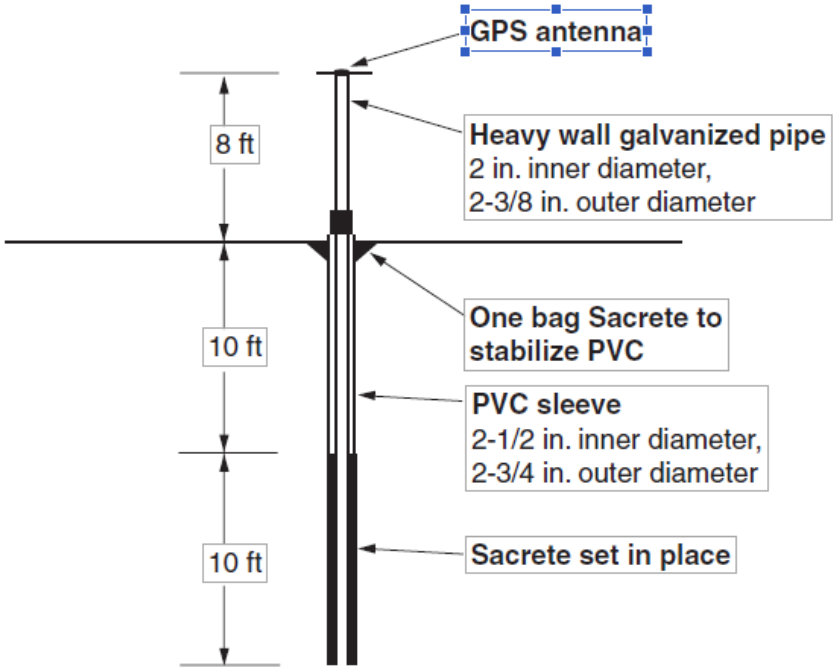

Figure 3-5 Schematic of a Port-A-Measure (PAM) monument (modified from Zilkoski and others, 2003)

Figure 3-6 Photograph of PAM station #68 in operated by Brazoria County GCD

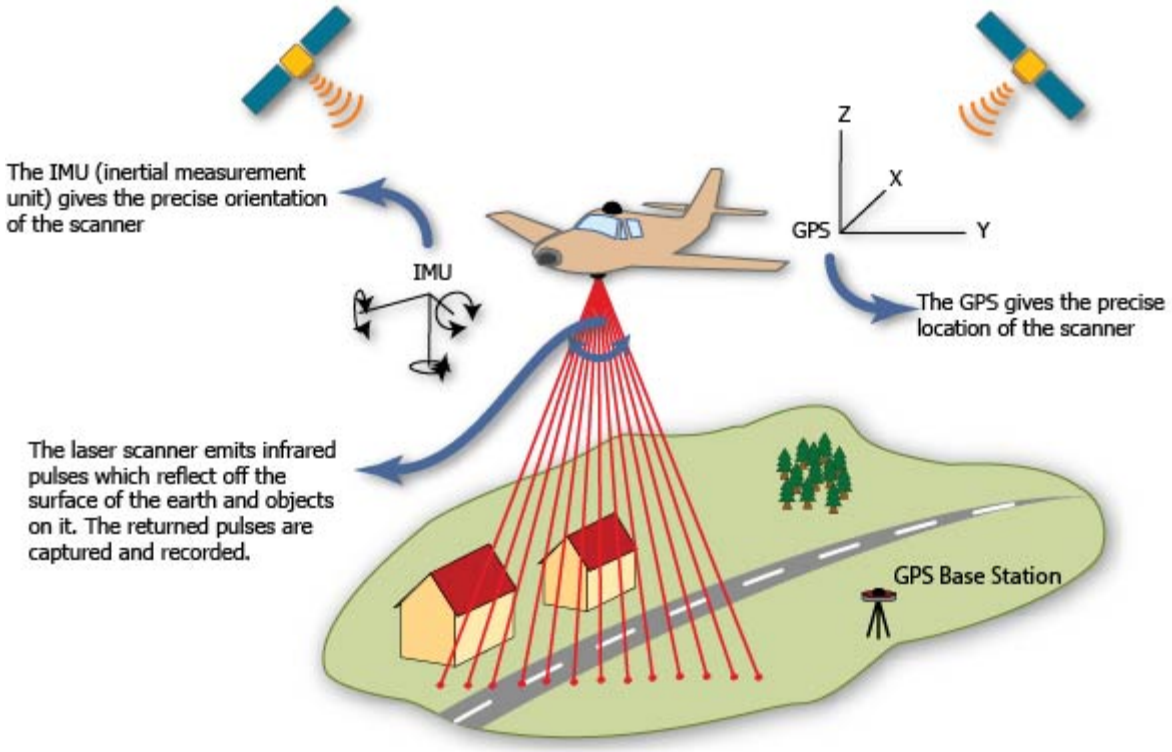

Figure 3-7 Components of Airborne LiDAR System (from http://gmv.cast.uark.edu/scanning-2/airborne-laser-scanning/)

4.0 RECOMMENDED APPROACH FOR MONITORING LAND SUBSIDENCE IN VICTORIA COUNTY

This section describes a recommended approach for monitoring land subsidence in Victoria County. The project consists of two phases that are intended to be performed in series. Phase 1 involves mapping historical subsidence using available SAR data. Phase 2 involves installing PAM stations. The decision to conduct Phase 2 is contingent on the land subsidence maps produced as part of the Phase 1 work. The estimated cost for the recommended work for Phase 1 and Phase 2 is $65,000.

4.1 Phase 1 – Mapping of Historical Subsidence using InSAR

Our initial review of available SAR data for Victoria County indicates that data are available for the following periods: mid-1990s to 2000; 2007-2011, and 2015-present. As part of Phase 1, the available data would be downloaded and evaluated. Based on the quality and coverage across Victoria County, the InSAR data will be analyzed for the purpose of generating maps of land subsidence. For each of the three time periods, at least one map of calculated land subsidence will be produced. Where the data supports time intervals that are less than 4 years, multiple maps of land subsidence will be produced for each of the three time intervals.

The estimated time to completed Phase 1 is four months. The estimated cost to complete Phase 1 is $20,000. Approximately $14,000 is for the analysis, and $6,000 is for generating a report and GIS files.

Among the issues that will be investigated after the land subsidence maps have been generated is whether oil and gas production in the Catahoula and Yegua-Jackson formations has caused land subsidence. The purpose of investigation is to generate information that will help prevent incorrectly attributing land subsidence to groundwater pumping where in fact, oil and gas pumping has been the primary cause of observed land subsidence. Two reports (Ratzlaff, 1982; Kreitler and others, 1988) have indicated this oil and gas production has caused land subsidence in Victoria County.

Ratzlaff (1982) concludes that land subsidence along the Texas coast was caused mostly by groundwater withdrawal; however, he identified locations where hydrocarbon production likely contributed to land subsidence. Ratzlaff (1982) used three criteria to identify where pumping of oil and gas is likely contributing to land subsidence. These three criteria are: (1) land subsidence has been measured; (2) historical groundwater pumping is insufficient to have caused land subsidence; and (3) historical hydrocarbon production has been sufficiently large enough to cause land subsidence. Among the locations where all three of these conditions are met is southeast Victoria County.

Kreitler and others (1988, 1990) report large-magnitude, widespread depressurization beneath the Texas coastal plain in the 1.2 to 2.4 kilometer (km) depth range as a result of production of hydrocarbons and associated brines. Pressure gradients calculated by Kreitler and others (1990) from bottom-hole pressure measurements in thousands of wells were substantially below expected normal hydrostatic pressure gradients within the depths of fluid production. Analysis of the bottom hole pressures indicate that depressurization of over several thousand feet of hydraulic head occur at some oil and gas fields in the Catahoula Formation, which underlies the Jasper Aquifer. Such large depressurization is expected to cause some land subsidence based on calculations presented by Sharp and Germait (1990) exist. At a depths from about 4,000 to 6,000 ft below ground surface, Kreitler and others (1988) report hydraulic heads of 1500 to -2000 feet below sea level in the southwest, southeast, and central Victoria County.

4.2 Phase 2 – Installation of PAM Stations

After the completion of Phase 1, Phase 2 will start by reviewing maps of land subsidence generated by the analysis of InSAR data in Phase 1 and by Young (2016) for potential locations for PAM stations. Three initial PAM locations are proposed. The location of the three sites will be based on estimated historical land subsidence and anticipated locations for future groundwater pumping. The estimated cost to complete the Phase 2 work is $45,000. The schedule will be dependent of siting the PAM locations and obtaining the necessary leases and right of ways.

Table 4-1 breaks out of the estimated Phase 2 cost of $45,000. The Phase 2 cost do not include all of the supporting activities that the District will need to conduct Phase 2. The District should meet with either FBSD, HGSD, or BCGCD to learn about the installation and operation of PAM stations prior to finalizing the site locations for the PAM stations. The budget also presumes that the District will perform the bulk of the data collection. The training budget is primarily to fund personnel who may be accompanying District personnel to the PAM stations at the on set of the data gathering activities.

Table 4-1 Estimated Costs Associated with the Installation and Operation of Three PAM Sites.

Task		Estimated Cost
ID	Description	
1	Siting PAM Stations	$3,000
2	Installation of Three PAM Stations	$21,000
3	GPS Equipment for Recording at a PAM Station	$7,000
4	Training and six month data collection	$5,000
5	Reporting and Meetings	$9,000
	Total	$45,000

5.0 REFERENCES

American Geophysical Union, 1984, Guidebook to studies of land subsidence due to ground-water withdrawal: Chelsea, Michigan, UNESCO, 305 p.

Bawden, G.W., Johnson, M.R., Kasmarek, M.C., Brandt, Justin, and Middleton, C.S., 2012, Investigation of land subsidence in the Houston-Galveston region of Texas by using the Global Positioning System and interferometric synthetic aperture radar, 1993–2000: U.S. Geological Survey Scientific Investigations Report 2012–5211, 88 p.

Bawden, G.W., Sneed, Michelle, Stork, S. V., and Galloway, D. L., 2003, Measuring human-induced land subsidence from space: U.S. Geological Survey Fact Sheet 069–03, 4 p.

Borchers, J. W, and Carpenter, M., 2014. Land Subsidence from Groundwater Use in California. Prepared by Luhdorff & Scalmanini Consulting Engineers,. For California Water Foundation

Buckley, S.,M. 2003 Land subsidence in Houston, Texas, measured by radar interferometry and constrained by extensometers. J. Geophys. Res., 108 (B11) (2003), p. 2542, 10.1029/2002JB001848

Casu, F., Buckley, S.M., Manzo, M., Pepe, A., Lanari, R., 2005. Large scale InSAR deformation time series: Phoenix and Houston case studies. In: International Geoscience and Remote Sensing Symposium (IGARSS). vol. 7. IEEE, pp. 5240–5243.

Chaussard, E., Bürgmann, R., Shirzaei, M., Fielding, E., & Baker, B. (2014). Predictability of hydraulic head changes and characterization of aquifer‐system and fault properties from InSAR‐derived ground deformation. Journal of Geophysical Research: Solid Earth, 119, 6572–6590.

Chen, J., Knight, R., & Zebker, H. A. (2017). The temporal and spatial variability of the confined aquifer head and storage properties in the San Luis Valley, Colorado inferred from multiple InSAR missions. Water Resources Research, 53, 9708–9720. https://doi.org/10.1002/ 2017WR020881

Coplin, L.S., and Galloway, Devin, 1999, Houston-Galveston, Texas—Managing coastal subsidence, *in* Galloway, Devin, Jones, D.R., and Ingebritsen, S.E., eds., Land subsidence in the United States: U.S. Geological Survey Circular 1182, p. 35–48.Domenico, P.A. and F.W. Schwartz. 1990. Physical and chemical hydrogeology: New York, NY, John Wiley & Sons, Inc., 824 p.

Engelkemeir, R. E., Khan, S. D., & Burke, K. (2010). Surface deformation in Houston, Texas using GPS. Tectonophysics, 490, 47-54.

European Space Agency, 2007, InSAR Principles—Guidelines for SAR interferometry processing and interpretation (ESA TM-19): The Netherlands, European Space Agency, 48 p.

Fowler, R. (2001). Topographic LIDAR, In Digital Elevation Model Technologies and Applications: The DEM Users Manual. (D. Maune, Ed.) The American Society for Photogrammetry and Remote Sensing, 207-236.

Freeze, R.A. and J.A. Cherry, J.A. 1979. Groundwater: Englewood Cliffs, N.J. Prentice Hall, 604 pp.

Furnans, J. Keester, M., Colven, D., Bauer, J., Barber, J., Gin, Gary., Danielson, V., Erickson, L., Ryan, R., Khorzad, K., Worsley, A., and Synder, G., ., 2017. Final Report: Identification of the Vulnerability

of the Major and Minor Aquifers of Texas to Subsidence with Regard to Groundwater Pumping., Texas Water Development Board TWDB Contract Number 1648302062.

Gabrysch RK (1984) Case History No. 9.12. The Houston-Galveston Region, Texas, U.S.A. In: Poland JF (ed) Guidebook to studies in land subsidence due to ground-water withdrawal. United Nations Educational, Scientific, and Cultural Organization, Chelsea, pp 253–262

Gabrysch, R. K. and R. J. Neighbors. 2005. Measuring a Century of Subsidence in Houston-Galveston Region, Texas: U.S., in Seventh International Symposium on Land Subsidence, Shanghai, China, October 23-28, 2005, Proceedings 379-387.

Gabrysch, R.K. 1982. Ground-Water Withdrawals and Land-Surface Subsidence in the Houston-Galveston Region, Texas, 1906—1980. United States Geological Survey Open-File Report 82-571, 68 p.

Gabrysch, R.K. and L.S. Coplin. 1990. Land-Surface Subsidence Resulting from Ground-Water Withdrawals in the Houston-Galveston Region, Texas, Through 1987. Report of Investigations No. 90-01, U.S. Geological Survey in cooperation with the Harris-Galveston Coastal Subsidence District.

Gabrysch, R.K. and R. J. Neighbors. 2000. Land-Surface Subsidence and its Control in the Houston-Galveston Region, Texas, 1906-1995: Proceedings of the Sixth International Symposium on Land-Surface Subsidence, Ravenna, Italy, September 24-29, p81-92.

Galloway, D., Jones, D., and Ingebritsen, S.: Land subsidence in the United States, USGS Circular 1182, US Geological Survey, Reston, VA, 35–48, 1999.

Hodgson, M.E. and Bresnahan, P., 2004, Accuracy of airborne lidar-derived elevation: empirical assessment and error budget: Photogrammetric Engineering & Remote Sensing, v. 70, no. 2, p. 331-339

Hoffmann, J., Zebker, H. A., Galloway, D. L., & Amelung, F. (2001). Seasonal subsidence and rebound in Las Vegas Valley, Nevada, observed by synthetic aperture radar interferometry. Water Resources Research, 37(6), 1551–1566. https://doi.org/10.1029/ 2000WR900404

Karacy, A., 2013. Subsidence Study in Northwest Harris County Using GPS, LIDAR, and INSAR Techniques, Thesis, Department of Earth and Atmospheric Sciences, University of Houston, May, 2013.

Kasmarek, M., Gabrysch, R., and Johnson, M.: Estimated land surface subsidence in Harris County, Texas, 1915–1917 to 2001, USGS Sci. Invest. Map 3097, 2 sheets, US Geological Survey, Reston, available at: http://pubs.usgs.gov/sim/3097/ (last access: 5 October 2015), 2009.

Kasmarek, M.C., Johnson, M.R., and Ramage, J.K., 2014, Water-level altitudes 2014 and water-level changes in the Chicot, Evangeline, and Jasper aquifers and compaction 1973–2013 in the Chicot and Evangeline aquifers, Houston-Galveston region, Texas: U.S. Geological Survey Scientific Investigations Map 3308, 20 p., 16 sheets, accessed February 10, 2018, at https://dx.doi.org/10.3133/sim3308.

Kearns, T. J., Wang, G., Bao, Y., Jiang, J., and Lee, D.: Current Land Subsidence and Groundwater Level Changes in the Houston Metropolitan Area, Texas (2005–2012), J. Surv. Eng., 05015002, 1–16, 2015.

Khan, S.D., Huang, Z., and Karacay, A., 2014. Study of ground subsidence in northwest Harris County using GPS, LiDAR, and InSAR techniques. Natural Hazards. Vol 73 (3) pg 1143-1173.

Kreitler, C.W., M.S. Akhter, A.C. Donnelly, and W.T. Wood. 1988. Hydrogeology of Formations Used for Deep-Well Injection, Texas Gulf Coast: Prepared for the USEPA by the Bureau of Economic Geology, University of Texas, Austin.

Kreitler, C.W., M.S. Akhter, and A.C.A. Donnely.1990. Hydrogeologic Hydrochemical Characterization of Texas Frio Formation Used for Deep-Well Injection of Chemical Wastes. Environ Geol Water Sci 16:107-12.

Meinzer, O.E. 1928. Compressibility and elasticity of artesian aquifers: Economic Geology, v. 23, no. 3, p. 263-291.

Meinzer, O.E. and H.A. Hard. 1925. The artesian-water supply of the Dakota sandstone in North Dakota with special reference to the Edgeley Quadrangle: U.S. Geological Survey Water-Supply Paper 520-E, p. 73–95.

Miller, M. M., and Shirzaei, M., 2019. Land Subsidence in Houston correlated with flooding from Hurricane Harvey. Remote Sensing Environment 223 , pg 368-378

National Oceanic and Atmospheric Administration (NOAA) Coastal (Service) Center. (2008). Lidar101 : An Introduction LiDAR Technology, Data, and Applications United States. Washington: National Academy Press.

National Research Council, 1991, Mitigating losses from land subsidence in the United States: Washington, D'. C., National Academy Press, 58 p.

Neighbors, R. J., and Mitchell, G. J. (2010). A plan to use continuously operating GPS stations to monitor subsidence in the Harris-Galveston coastal subsidence district. Retrieved 11, 2012 from the National Geodetic Survey and Harris Galveston Subsidence District. http://www.ngs.noaa.gov/PUBS_LIB/A_PlanToUseContinuouslyOperatingGPS_%20StationsToMonitorSubsidenceInTheHarrisGalvestonCoastalSubsidenceDistrict.pdf

Osmanoglu, B.; Dixon, T.H.; Wdowinski, S.; Cabral-Cano, E.; Jiang, Y. Mexico city subsidence observed with persistent scatter InSAR. Int. J. Appl. Earth Obs. Geoinf. **2011**, 13, 1–12.

Pratt, W.E., and Johnson, D.W., 1926, Local subsidence of the Goose Creek oil field: Journal of Geology, v. 34, p. 577–590.

Qu, F., Lu, Z., Zhang, Q., Bawden, G.W., Kim, J.W., Zhao, C., Qu, W., 2015. Mapping ground deformation over Houston-Galveston, Texas using multi-temporal InSAR. Remote Sens. Environ. 169, 290–306. https://doi.org/10.1016/j.rse.2015.08.027

Ratzlaff, K.W., 1982. Land-Surface Subsidence in the Texas Coastal Region: Texas Department of Water Resources Report 272, 26 p.

Reeves, J. A., Knight, R., Zebker, H. A., Schreüder, W. A., Shanker Agram, P., & Lauknes, T. R. (2011). High quality InSAR data linked to seasonal change in hydraulic head for an agricultural area in the San Luis Valley, Colorado. Water Resources Research, 47, W12510. https://doi.org/10.1029/2010WR010312

Revil, A., D. Grauls, and O. and Brevart. 2002. Mechanical Compaction of sand/clay mixtures. Journal of Geophysical Research, Vol 107, No. B11. P. 11-1 to 11-15.

Seifert, J. and C. Drabek. 2006. Chapter 13: History of Production and Potential Future Production of the Gulf Coast Aquifer, in Aquifers of the Gulf Coast, Texas Water Development Board Report 365, Austin, Texas

Sharp J.M. and S.J. Germait. 1990. Risk assessment and causes of subsidence along the Texas Gulf Coast. In: (Fairbridge, R.W., and Paepe., eds.) Proceedings of NATO Conference on the Greenhouse Effect, Sea Level and Drought. Kluwer Academic Publishers, Dordrecht.

Sithole, G., & Vosselman, G. (2004). Experimental comparison of filter algorithms for bare-Earth. Journal of Photogrammetry & Remote Sensing, 59, 85-101.

Smith, R. G., Knight, R., Chen, J., Reeves, J. A., Zebker, H. A., Farr, T., & Liu, Z. (2017). Estimating the permanent loss of groundwater storage in the southern San Joaquin Valley, California. Water Resources Research, 53, 2133–2148. https://doi.org/10.1002/2016WR019861

Smith, R., & Knight, R. (2019). Modeling land subsidence using InSAR and airborne electromagnetic data. Water Resources Research, 55, 2801–2819. https://doi.org/10.1029/ 2018WR024185

Sneed, M., Brandt, J. and M. Solt, 2013, Land Subsidence along the Delta-Mendota Canal in the Northern Part of the San Joaquin Valley, California, 2003-2010. US Geological Survey Scientific Investigations Report 2013-5142, 87 p.

Wang, G. and T. Soler. 2014. Measuring Land Subsidence Using GPS: Ellipsoid Height vs. Orthometric Height, J. Surv. Eng., 141, 1– 12, 2014.

Wang, G., J. Welch, T.J. Kearns, J. Yang, and J. Serna. 2015. Introduction to GPS geodetic infrastructure for land subsidence monitoring in Houston Texas, USA. Proceedings, IAHS, 372. P. 297-303.

Young, S., 2016. Estimates of Land Subsidence in GMA 15 Based on Ground Surface Elevation Data and Model Results, Prepared for Calhoun County GCD, Coastal Bend GCD, Coastal Plains GCD, Pecan Valley GCD, Refugio County GCD, Texana GCD, and Victoria County GCD, prepared by INTERA Inc., Austin, TX.

Zilkoski, D. B., L. Hall, G. Mitchell, V. Kammula, A. Singh, W. Chrismer, and R. Neighbors. 2003. The Harris-Galveston coastal subsidence district/national geodetic survey automated global positioning system subsidence monitoring project, Proc., US Geological Survey Subsidence Interest Group Conf., Galveston, Texas, 27–29 November 2001, USGS OpenFile Report, 03–308, 13–28, 2003.

Zilkoski, D.B., Hall, L.W., Mitchell, G.J., Kammula, V., Singh, A., Chrismer, W.M., and Neighbors, R.J. (2001). The Harris-Galveston Coastal Subsidence District/National Geodetic Survey Automated Global Positioning System Subsidence Monitoring Project. USGS Open-File Report 03-308, pp 13-26. http://www.hgsubsidence.org/assets/pdfdocuments/GPSProject.pdf

Appendix A

Measuring Human-Induced Land Subsidence from Space

(United States Geological Survey Fact Sheet 069-03)

USGS
science for a changing world

Measuring Human-Induced Land Subsidence from Space

Satellite Interferometric Synthetic Aperture Radar (InSAR) is a revolutionary technique that allows scientists to measure and map changes on the Earth's surface as small as a few millimeters. By bouncing radar signals off the ground surface from the same point in space but at different times, the radar satellite can measure the change in distance between the satellite and ground (range change) as the land surface uplifts or subsides. Maps of relative ground-surface change (interferograms) are constructed from the InSAR data to help scientists understand how ground-water pumping, hydrocarbon production, or other human activities cause the land surface to uplift or subside. Interferograms developed by the USGS for study areas in California, Nevada, and Texas are used in this Fact Sheet to demonstrate some of the applications of InSAR to assess human-induced land deformation.

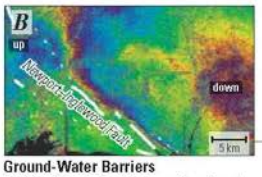

Ground-Water Barriers
Faults and geologic structures often impede the flow of ground water and can be recognized as linear InSAR features where ground-water levels decline on one side of the fault or rise on the other side of the fault

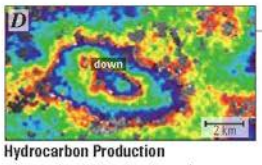

Hydrocarbon Production
The pumping of oil is often imaged as a "bull's-eye" feature, such as the 58 mm of subsidence measured in the Beverly Hills Oil Field (5 years: Oct. 1993–Oct. 1998)

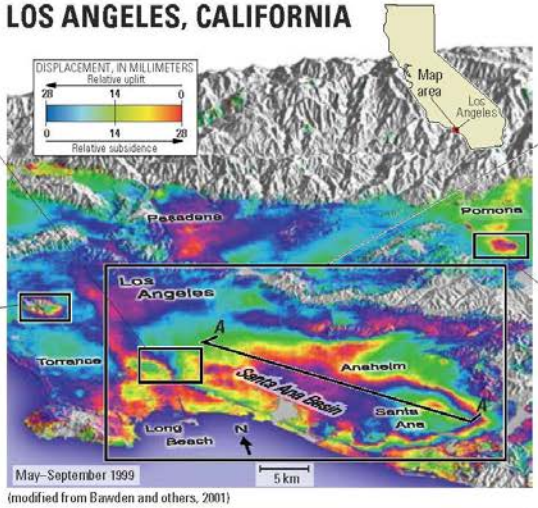

(modified from Bawden and others, 2001)

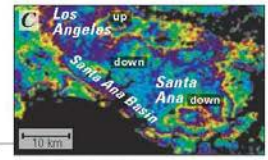

Multi-Year Subsidence
As water levels decline near Santa Ana, the land surface subsides at a rate of about 20 mm per year (Oct. 1993–Oct. 1998)

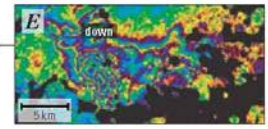

Localized Subsidence
More than 180 mm of ground-water-pumping induced subsidence (1993–95) resulted in cracked building foundations near Pomona

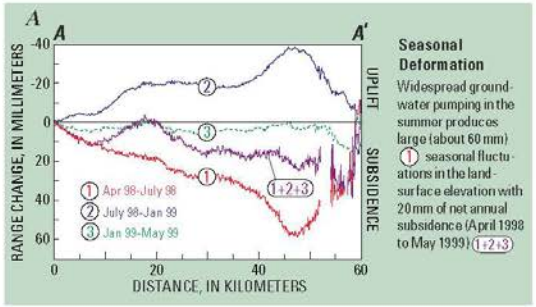

Seasonal Deformation
Widespread ground-water pumping in the summer produces large (about 60 mm) (1) seasonal fluctuations in the land-surface elevation with 20 mm of net annual subsidence (April 1998 to May 1999) (1+2+3)

How to read an interferogram:

1. *Count the number of InSAR fringes between two points on the interferogram, where one fringe is one complete color cycle (i.e. yellow, red, blue, green, yellow).*
2. *Multiply the number of fringes by 28.3 mm (1.1 in).*
3. *Determine if the ground moved closer (uplift) or farther away (subsidence) from the satellite by matching how the colors change between the two points with the InSAR scale bar. (i.e. yellow, red, blue, green shows relative subsidence).*

InSAR provides invaluable spatial information needed to assess and mitigate human-induced subsidence.

In metropolitan Los Angeles, InSAR imagery found widespread seasonal and annual human-induced surface deformation related to both ground-water and hydrocarbon production. The largest feature in the May–September 1999 interferogram (center) is the 40-km (kilometer) long Santa Ana Basin. Ground-water pumping and artificial recharge are producing as much as 60 mm (millimeter) of seasonal uplift and subsidence with 20 mm of net basin subsidence (April 1998–May 1999) (Fig. *A*). The Newport-Inglewood Fault bounds the southwest margin of the Santa Ana Basin; InSAR shows that there is about a 2-km offset between the mapped trace of the fault and the subsurface ground-water barrier (Fig. *B*). Many of the deformation features are long lasting (Fig. *C*) and can exhibit significant surface deformation as shown by the examples of hydrocarbon production in Beverly Hills (Fig. *D*) and property damage near Pomona (Fig. *E*). Additionally, the human-induced land deformation produces horizontal surface motion that obscures, and in some cases mimics, the tectonic signals expected from the blind thrust faults beneath Los Angeles (Bawden and others, 2001).

U.S. Department of the Interior
U.S. Geological Survey

Printed on recycled paper

Fact Sheet 069–03
December 2003

SANTA CLARA VALLEY, CALIFORNIA

Silicon Valley Subsides

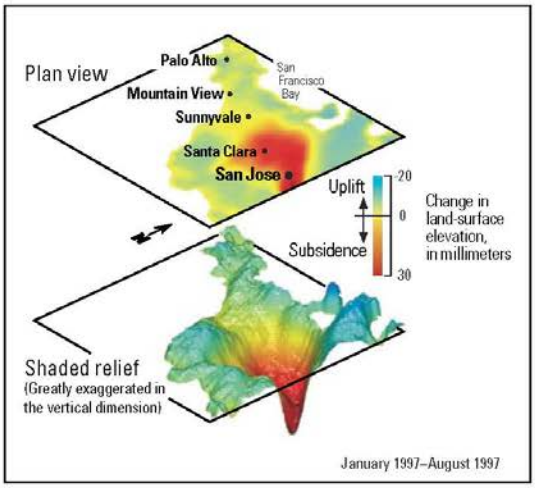

InSAR was used to evaluate seasonal and multi-year deformation patterns, which are critical for implementing appropriate water-management strategies that may include subsidence mitigation. Santa Clara Valley was the first area in the Nation (1940) where land subsidence (nearly 5 m) associated with ground-water withdrawal was recognized. A 5-year interferogram (Sept. 1992–Aug. 1997) shows a small amount (5–10 mm) of regional uplift. The uplift corresponds to a period of water-level recovery throughout the valley. An 8-month interferogram (Jan.–Aug. 1997) shows seasonal subsidence of about 30 mm near San Jose and corresponds to about a 10-m decline in water levels. The lack of subsidence between 1992–97 indicates that the seasonal subsidence was temporary (Galloway and others, 1999).

InSAR imagery identified new faults and geologic structures in the Santa Clara Valley. The ***A–A′*** cross section on the 8-month interferogram (bottom-right) shows that the location of the steep subsidence gradient is offset about 1 km from the mapped trace of the Silver Creek Fault. The USGS Earthquake Hazards Team conducted a seismic reflection/refraction survey across the InSAR feature and identified it as a previously unrecognized fault (Catchings and others, 2000).

5–10 millimeters of multi-year uplift

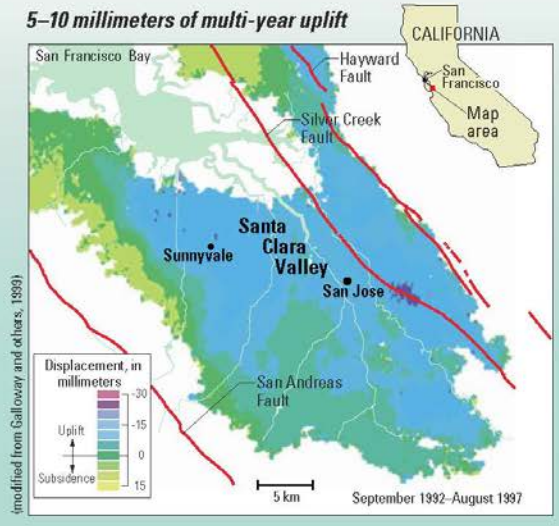

(modified from Galloway and others, 1999)

30 millimeters of seasonal subsidence

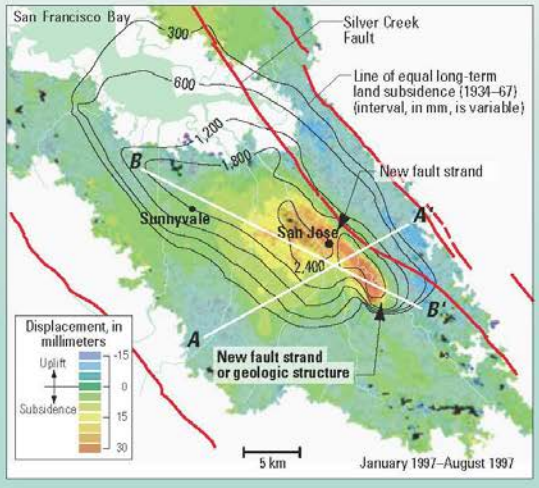

InSAR Finds New Fault Strand

The ***B–B′*** cross section (right) shows a steep subsidence gradient in an area where there are no mapped faults, revealing a previously unrecognized structure or fault that also acts as a ground-water flow barrier. Mapping faults and geologic structures in an aquifer system is crucial for understanding ground-water flow, regional subsidence patterns, and potential seismic hazards.

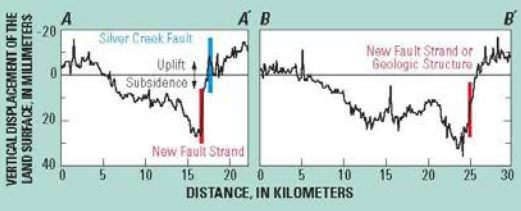

LAS VEGAS VALLEY, NEVADA

200 millimeters of multi-year subsidence

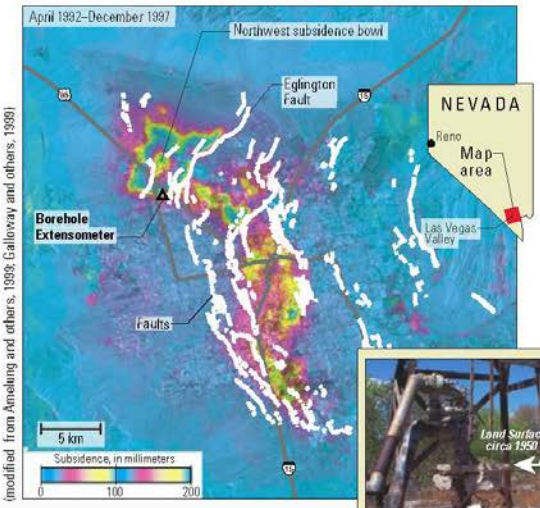

(modified from Amelung and others, 1999; Galloway and others, 1999)

This well in Las Vegas Valley now extends about 2 meters above the land surface because of subsidence.

Subsidence may also cause well casings in the subsurface to collapse and thereby damaging the well.

InSAR determined the spatial extent of subsidence and how the subsidence might affect urban development. Las Vegas Valley is one of the fastest growing areas in the Nation. Since the 1950s, ground-water pumping has resulted in water-level declines of more than 100 m. These large water-level declines have resulted in nearly 2 m of subsidence, which has caused fissures and damaged wells. A 5-year interferogram (Apr. 1992– Dec. 1997) (left) shows the full extent of the aquifer system and shows 190 mm of localized subsidence in a distinct bowl in the northwest part of the valley. The southeastern margin of the bowl is structurally controlled by the Eglington Fault.

A borehole extensometer (an instrument to measure aquifer-system compaction) was constructed in 1995 to precisely measure the subsidence. However, interferograms show that the maximum subsidence is located north of the extensometer site. If the InSAR imagery were available prior to extensometer construction, it may have been constructed in the area of maximum subsidence. While extensometers measure subsidence at only one location, InSAR measures subsidence at thousands of points.

ANTELOPE VALLEY, CALIFORNIA

InSAR and computer model roughly agree...

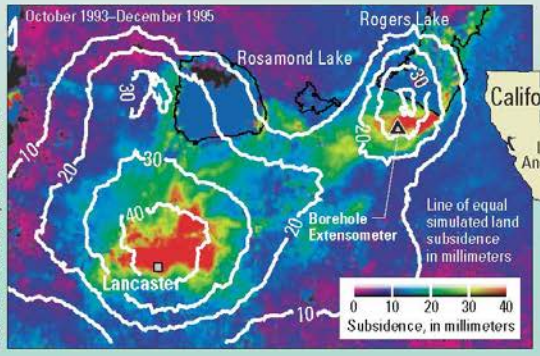

(modified from Galloway and others, 2000)

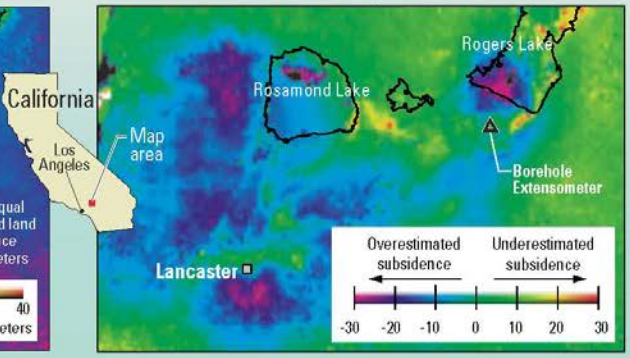

but residuals show added complexities

InSAR provides new techniques to calibrate scientific instrumentation and develop sophisticated ground-water models. Extensive pumping in Antelope Valley since the 1940s contributed to nearly 2 m of subsidence in Lancaster and more than 1 m south of Rogers Lake, Edwards Air Force Base. During 1993–95, InSAR measured about 40 mm of subsidence at an extensometer site in the Antelope Valley (upper left); the extensometer measured 31 mm. This disparity indicates that 20% of the subsidence occurred below the maximum depth of the extensometer (256 m). InSAR imagery was also used to evaluate a computer model that simulated land subsidence and ground-water flow. A residuals image (upper right) (InSAR observations subtracted from the modeled subsidence) shows that although the computer model simulated the subsidence reasonably well, it overestimated the subsidence in some areas. These results highlight the potential use of InSAR measurement to better constrain computer models of land subsidence (Galloway and others, 1998; Hoffmann and others, 2003).

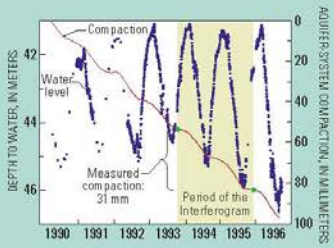

Additional examples of human-induced surface deformation measured with InSAR

Yucca Flat Nuclear Test Site, Nevada

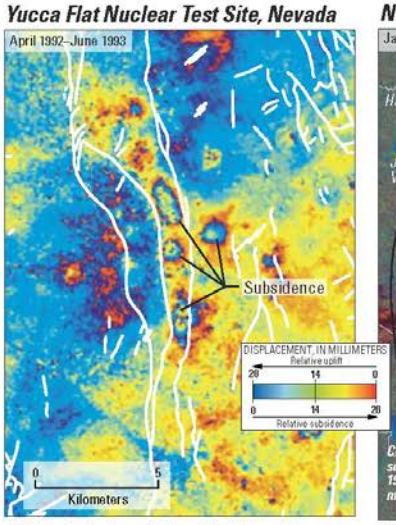

InSAR monitoring shows fault-controlled deformation from the dissipation of residual ground-water pore-fluid pressure changes in response to past underground nuclear weapons testing (R. Laczniak, U.S. Geological Survey, written commun., 2003).

NW Suburban Houston, Texas

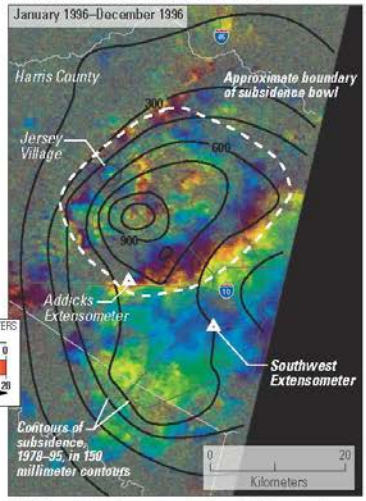

InSAR monitoring shows ground-water subsidence continues to follow historical patterns in the northwest Houston area.

Bakersfield, California

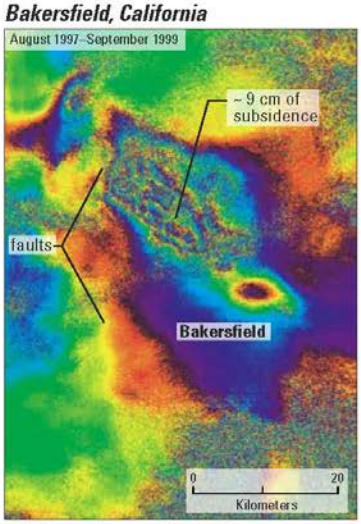

InSAR imagery shows a complex subsidence pattern associated with hydrocarbon extraction north of Bakersfield and shows that faults play a vital role in subsidence.

Advantages of InSAR

InSAR is ideally suited to measure the spatial extent and magnitude of surface deformation associated with fluid extraction and natural hazards (earthquakes, volcanoes, landslides). It is often less expensive than obtaining sparse point measurements from labor-intensive spirit-leveling and Global Positioning System (GPS) surveys and can provide millions of data points in a region about 10,000 square kilometers. By identifying specific areas of deformation within broader regions of interest, InSAR imagery can also be used to better position specialized instrumentation (such as extensometers, GPS networks, and leveling lines) designed to precisely measure and monitor surface deformation over limited areas.

Radar data used to produce the interferograms shown in this fact sheet were obtained from the European Space Agency, distributed through Eurimage Corporation for the purposes of research and development.

– G.W. Bawden, M. Sneed, S.V. Stork, and D.L. Galloway

Land subsidence measuring techniques

METHOD	Component displacement	Resolution[1] (millimeters)	Spatial density[2] (samples/survey)	Spatial scale (elements)
Spirit level	vertical	0.1–1	10–100	line-network
Geodimeter	horizontal	1	10–100	line-network
Borehole extensometer	vertical	0.01–0.1	1–3	point
Horizontal extensometer:				
Tape	horizontal	0.3	1–10	line-array
Invar wire	horizontal	0.0001	1	line
Quartz tube	horizontal	0.00001	1	line
GPS	vertical horizontal	20 5	10–100	network
InSAR	range	5–10	100,000–10,000,000	map pixel[3]

[1] Measurement resolution attainable under optimum conditions. Values are given in metric units to conform with standard geodetic guidelines. (One inch is equal to 25.4 millimeters and 1 foot is equal to 304.8 millimeters.)
[2] Number of measurements generally attainable under good conditions to define the spatial extent of land subsidence at the scale of the survey.
[3] A pixel on an InSAR displacement map is typically 30 to 90 square meters on the ground.

References

Amelung, F., Galloway, D.L., Bell, J.W., Zebker, H.A., and Laczniak, R.J., 1999, Sensing the ups and downs of Las Vegas—InSAR reveals structural control of land subsidence and aquifer-system deformation: Geology, v. 27, p. 483–486.

Bawden, G.W., Thatcher, W., Stein, R.S., Hudnut, K.W., and Peltzer, G., 2001, Tectonic contraction across Los Angeles after removal of groundwater pumping effects: Nature, v. 412, p. 812–815.

Catchings, R.D., Goldman, M.R., Gandhok, G., Rymer, M.J., and Underwood, D.H., 2000, Seismic imaging evidence for faulting across the northwestern projection of the Silver Creek Fault, San Jose, California: U.S. Geological Survey Open File Report 00–0125, 29 p.

Galloway, D.L., Hudnut, K.W., Ingebritsen, S.E., Phillips, S.P., Peltzer, G., Rogez, F., and Rosen, P.A., 1998, Detection of aquifer system compaction and land subsidence using interferometric synthetic aperture radar, Antelope Valley, Mojave Desert, California: Water Resources Research, v. 34, p. 2,573–2,585.

Galloway, D.L., Jones, D.R., and Ingebritsen, S.E., 1999, Land subsidence in the United States: U.S. Geological Survey Circular 1182, 175 p.

Galloway, D.L., Jones, D.R., and Ingebritsen, S.E., 2000, Measuring land subsidence from space: U.S. Geological Survey Fact Sheet 051–00, 4 p.

Hoffmann, J., Galloway, D.L., Zebker, H.A., 2003, Inverse modeling of interbed storage parameters using land subsidence observations, Antelope Valley, California: Water Resources Research, v. 39, no. 2, SBH 5.

For additional information on InSAR measured surface deformation, please contact:

Gerald Bawden (gbawden@usgs.gov)
U.S. Geological Survey — Placer Hall
6000 J Street
Sacramento, California 95819–6129
916–278–3131

http://ca.water.usgs.gov/insar
http://quake.wr.usgs.gov/research/deformation/modeling/socal/la.html